

INVESTIGATION OF THE EFFECTS OF SELECTED PHYSICAL FACTORS ON WATER COLLECTION EFFICIENCY OF AN AERODYNAMIC SURFACE IN ICING PROBLEMS

Janusz Sznajder

Instytut Lotnictwa (Institute of Aviation), Warsaw, Poland

E-mail: jsznaj@ilot.edu.pl

Abstract

A model of two-phase, low concentration water flow is presented. The developed computational method is dedicated to the determination of water collection efficiency of an aerodynamic surface. The implementation of flow boundary condition on the surface is in accordance with algorithms used for simulation of surface icing. The method has been implemented as an User-Defined-Function module in the FLUENT code solving RANS equations. The results of computations of the water collection efficiency have been compared with experimental data.

Key words: Aerodynamics, Computational Fluid Dynamics, Multi-phase Flows

INTRODUCTION

Simulation of atmospheric icing effects on a general, three-dimensional surface involves the solution of several separate problems, such as: determination of two-phase flow field around the surface including air- and water-droplet flow, solution of parameters of water film on the surface: distribution of its height and velocity, and determination of heat fluxes reaching the surface including heat incoming with the water droplets, heat resulting from friction in the boundary layer, heat created through phase changes and heat conducted from underneath the surface. Due to the complexity of the problem, it is usually divided into sub-problems analysed sequentially as separate tasks, using separate numerical tools, each dealing with an element of the physical phenomenon, which is the ice accretion on the surface and its effects on the aerodynamic characteristics. The typical composition of numerical tools and the flow of information is shown in Figure 1.

The aim of this paper is to present the details of the assumed method of determination of collection efficiency of a surface in two-phase flow, consisting of air and dispersed water droplets, and some examples of its practical application. It is assumed, that the amount of water in the flow, measured by the Liquid Water Content parameter is similar as in typical, real conditions of atmospheric icing.

Two approaches are generally used in numerical computations of this quantity. Chronologically the first of them is an Lagrangian approach [1], tracking the motion of a droplet in space. It requires the determination of a "source zone" of water droplets hitting the surface. By the evaluation of the trajectories of individual droplets leaving the source zone it is possible to determine the local collection efficiency as the ratio of the distance between the source points of two closest droplets in the source zone (far field) and the distance of their impact points along the airfoil surface. This approach was popular in the first ice accretion simulation codes using potential model of air flow, such as LEWICE [1]. Its constraints appear in the application for multi-element airfoils and three-dimensional surfaces, where the source zones for droplets reaching wing surface have more complicated shape than the source zones in the two-dimensional, single-element airfoil case. In recent years, particularly in the

last decade, the task of determination of water collection efficiency is fulfilled more often using an Eulerian approach [2]. In this approach water dispersed in droplets is regarded as a continuous phase and the solution of droplet motion is being obtained simultaneously for all points of the computational domain. In this approach there is no need for the determination of the source zone for droplets hitting the surface. Instead, the droplet flow field is determined simultaneously in the whole computational domain by the solution of the continuity and momentum equations for the droplet phase with appropriate boundary and initial conditions. This approach is analogous to the determination of air flow field using Euler or RANS equations of Fluid Dynamics and became competitive to the Lagrangian approach as the solutions of Euler and RANS equations became affordable means of solving practical design problems in the industry. In many cases the solution of air and water flow is being conducted using different computational codes. This is done on the grounds of the frequently adopted assumption that the droplet flow does not affect the air flow, which is true for low water concentration [2]. Applying this assumption it is possible to conduct a solution of water flow for a steady case using a converged, steady solution of air flow. In the present approach similar assumption regarding the one-directional influence of air flow on droplet flow was applied. Based on this assumption a model of two-phase flow with boundary conditions for external flow was built and implemented in the FLUENT (ANSYS) solver as the User-Defined-Function module.

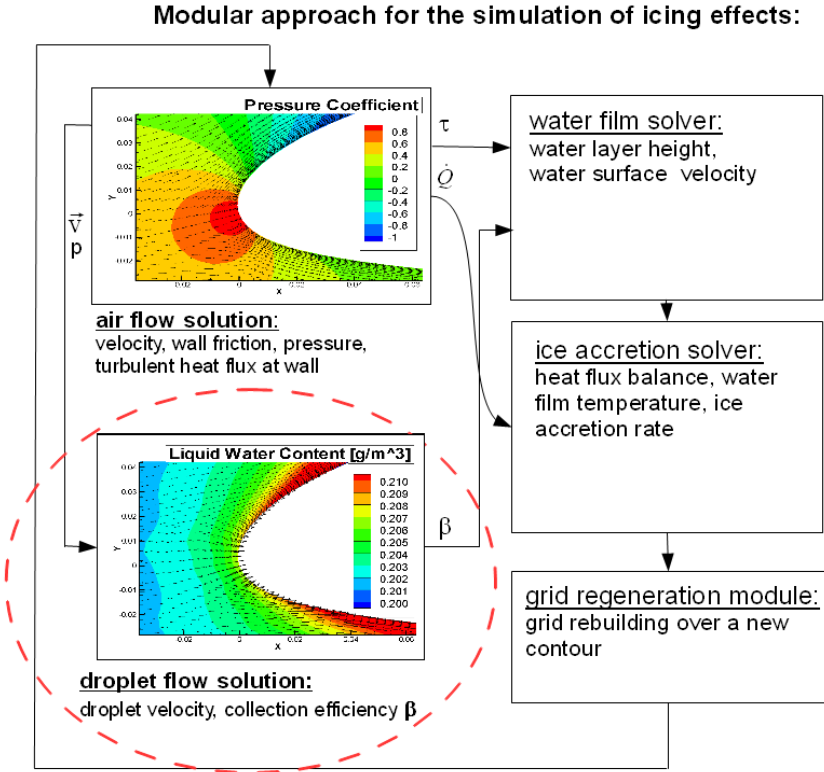


Figure 1 Partitioning of the method of simulation of icing effects into sub-problems analysed with different numerical tools

The results of the droplet flow model form input to another modules of the icing effects simulation model, which is currently under development. There are also some important questions regarding the amount of water captured by the surface that are worth investigating from the point of view of aviation safety. They include the effect of flight parameters such as speed or angle of attack on the mass and surface distribution of the collected water, or the

effect of a model of droplet dispersion in terms of droplet size on the mass and surface distribution of the collected water. This paper addresses these issues.

FLOW EQUATIONS

The model of air flow applied in the present approach is described with equations of conservation of mass, momentum and energy supplemented by turbulence equation (one-equation Spalart-Almaras turbulence model). The system of equations is solved by the FLUENT solver [3] in identical way as in the case of one-phase fluid flow. For the present work the pressure-based solver was selected with second order upwind discretization of flow variables and SIMPLE-type pressure-velocity coupling.

The water-droplet-phase flow is described with the continuity equation:

$$\frac{\partial \rho_d}{\partial t} + \nabla \cdot (\rho_d \vec{U}_d) = 0, \quad (1)$$

and the momentum conservation equation, written in the following, conservative form:

$$\frac{\partial \rho_d \vec{U}_d}{\partial t} + \nabla \cdot (\rho_d \vec{U}_d) \vec{U}_d = \vec{f}_d + \rho_d \left(1 - \frac{\rho_a}{\rho_w}\right) \vec{g} - \frac{\rho_d}{\rho_w} \cdot \nabla p \quad (2)$$

where:

\vec{U}_d - droplet velocity,

ρ_d - droplet phase density, equal to $\alpha \cdot \rho_w$,

α - droplet phase volume fraction,

ρ_w - water density,

ρ_a - air density,

\vec{f}_d - drag force

\vec{g} - gravitational acceleration.

The first terms on the left side of equations (1) and (2) describe unsteady phenomena and are omitted in the implementation of steady flow case. The divergence terms are treated as follows. For steady-flow cases the FLUENT solver provides the possibility of computing the transport of a user-defined scalar ϕ_k solving the equation written in the following general form:

$$\nabla \cdot (\vec{\psi} \phi_k - \Gamma_k \cdot \phi_k) = S_{\phi_k} \quad (3)$$

where $\vec{\psi}$ is a vector field and Γ_k diffusion coefficient of the scalar “k”. In the default case $\vec{\psi} = \rho \vec{U}$, where \vec{U} is the primary-phase fluid velocity.

In the present, two-dimensional case, three scalars have been used to represent three variables: ρ_d , u_d , and v_d , where u_d and v_d are components of the droplet velocity \vec{U}_d . For each of them Equation (3) is solved in the computational domain. The components of the $\vec{\psi}$ vector are the products $\rho_d u_d$ and $\rho_d v_d$. The scalar Γ in Equation (3) is set to zero, in order to comply with Equations (1) and (2). The computation of the advection terms in equation (1) and (2) is being accomplished in an user-defined procedure, integrating the advection term in equation (3) over the cell volume. This is done applying Gauss Divergence Theorem. The wall values of the $\vec{\psi}$ vector components are computed using an upwind scheme, based on cell centre

values and gradients of scalars computed at the cell centres. For the boundary cells the wall values of the scalars are set as boundary conditions.

The forces acting on the droplets taken into account include droplet drag, the net effect of gravity and buoyancy, and effect of pressure gradient in the flow field. This is what most researches take into account, e.g. [2,4]. Drag force is computed using formula proposed by Morrison[5] for a sphere, because of reported agreement with experimental data for a wide range of droplet Reynolds number (Figure 1). The values of Reynolds number encountered in the computation of droplet drag usually don't exceed 100, but it is mentioned in the literature [2], that in some special cases, with large droplet diameters and unconverged solution, Reynolds number of a droplet may reach a value of 1000. It is recommended, that for fast convergence adequate drag formula be used. Drag force per unit volume is evaluated by multiplying drag of a single droplet (sphere) by the factor $\frac{\rho_d}{V_d \cdot \rho_w}$, where V_d is droplet volume.

$$c_D = \frac{24}{Re} + \frac{2.6 \cdot \frac{Re}{5}}{1 + \left(\frac{Re}{5}\right)^{1.52}} + \frac{0.411 \left(\frac{Re}{263000}\right)^{-7.94}}{1 + \left(\frac{Re}{263000}\right)^{-8}} + \left(\frac{Re^{0.8}}{461000}\right) \quad (4)$$

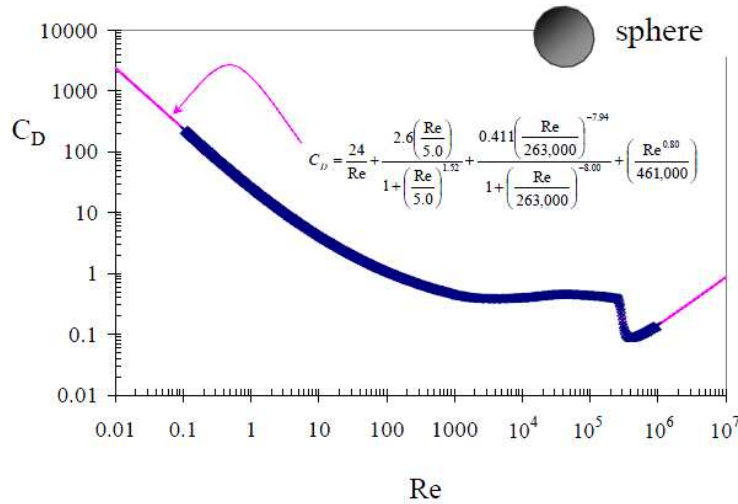


Figure 1. Comparison of analytical formula for droplet c_D with experimental data [5].

The Equations (1) and (2) represent a model of one-directional coupling in a two-phase flow, where the second phase flow does not influence the main phase flow. This assumption is commonly used for water concentration found in atmospheric icing problems [2,4].

Collection efficiency, β at a point of a surface is computed as:

$$\beta = \frac{\rho_d \bar{U}_d \cdot \bar{n}}{\rho_{d \text{ inf}} \cdot |\bar{U}_{d \text{ inf}}|} \quad (5)$$

where \bar{n} is a local surface normal vector, and $\rho_{d \text{ inf}}$ is droplet phase density, referred to also as Liquid Water Content (LWC).

Boundary conditions for the droplet flow have been chosen to correspond to the external flow boundary conditions being used for the computation of the aerodynamic characteristics of airfoils and three-dimensional bodies. The external boundary surfaces of the computational domain have been divided into two categories: pressure far-field and pressure outlet. The pressure far field includes surfaces of uniform and undisturbed flow lying ahead of and on both sides of the airfoil. The air flow quantities being set there include Mach number, X and Y components of the vector of the flow direction, pressure and temperature. They allow for the determination of the values of the flow variables computed by the solver: components of flow velocity, density, pressure and temperature. The water flow variables include mass concentration and X and Y components of the droplet velocity. It is assumed that the X and Y components of the air and water droplet velocity are equal in the far field (The computational problem may be considered as body moving through a two-phase fluid at rest). On the outlet surface only the pressure and temperature are set. The air flow velocities and density include disturbances caused by the airfoil and are computed by the solver. Similarly the water flow concentration and velocity components are computed up to the cell center point adjacent to the outlet surface. Their values on the outlet surface are extrapolated using gradients computed in the centre of the cell.

On the airfoil surface the typical wall no-slip boundary condition is applied for the air flow. For the water flow there are two cases treated in different way: the case when water is intercepted by the surface and the case when water droplets move by the surface. In the first case, when $(\vec{U}_d \cdot \vec{n}) < 0$, \vec{n} being the cell-wall normal vector, the airfoil surface is considered totally permeable for the water. The water velocity on the surface is extrapolated using gradients computed in the cell centre. This is a standard procedure applied for the computation of collection efficiency for the simulation of ice accretion. The flow of water on the surface is a separate problem, being treated in the ice accretion simulation codes with the application of heat exchange and heat balancing procedure, summing heat flows in and out of the surface. This allows for the determination of the amount of water that freezes in particular location or runs away along the surface. Such procedure has not been created for the present work yet, but is planned for the future.

In the case when $(\vec{U}_d \cdot \vec{n}) > 0$ the water concentration on the surface, ρ_d is set to zero, and the components of water flow velocity are extrapolated using gradients computed at the cell center. This ensures the continuity of droplet flow variables.

RESULTS OF COMPUTATIONS

In order to compare the present method with experimental results, two computational cases were created using NACA 23012 airfoil of chord equal 0.9144m, at the angle of attack $\alpha=2.5^\circ$. Free stream velocity was 78.23m/s, far field pressure and temperature was 101330Pa and 299K respectively. In the first case Liquid Water Content (LWC, equal to ρ_d far away from the airfoil) was set at 0.19g/m^3 and medium droplet diameter was $20\mu\text{m}$. In the second case LWC was 1.89g/m^3 and droplet diameter $236\mu\text{m}$. The experimental results were reported in [6] and quoted in [4] and represented measured distribution of collection efficiency of a set of droplet sizes with Median Volumetric Diameter of $20\mu\text{m}$ and $236\mu\text{m}$. The computed characteristics of airfoil collection efficiency is shown in Figure 2. The computations were performed on a mesh of 25000 elements. In the vicinity of the airfoil boundary layer structured mesh was created, with the $y+$ parameter value ≥ 30 over most of the airfoil surface. Further away from the surface mesh was of “pave” type with quadrilateral elements. Figure 2 shows the comparison of the results of the present method with the experimental results of [6]. The results of the present method were obtained for two cases: for a case with

water phase composed of droplets of single diameter of $20\mu\text{m}$, and for a normal distribution of droplet diameter, with medium diameter $\mu=20\mu\text{m}$ and standard deviation $\sigma=6.6(6)$ (1/6 of droplet diameter range). The droplet diameter range was divided into 11 zones, each with single, medium droplet diameter in the zone. The reported droplet distribution in experiment[4] is roughly similar, but with 9 diameter zones.

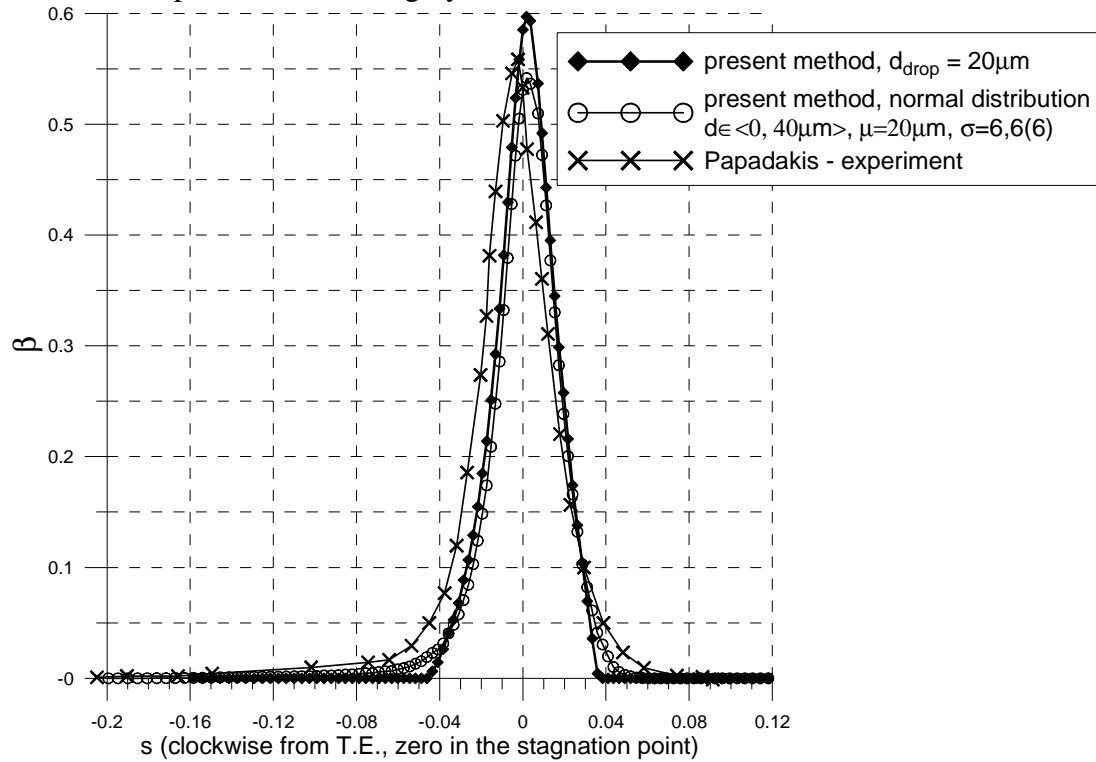


Figure 2. Distribution of the water collection efficiency along the airfoil circumference, first test case.

The overall agreement between the experimental and computational results is good, especially the maximum value of β computed for normal distribution of droplet diameter is very close to the value obtained in experiment. The main differences between the computational and experimental results are the shift of the computed characteristics to the right (into the suction zone) and underprediction of β in the areas of low β . The shift of the computed β characteristic may be justified by the inertia of droplets, preventing them to follow air flow and hit the surface in the stagnation point at right angle (as the reported experiment data with maximum β in the stagnation point suggests). The underprediction of β , especially away from the stagnation point may suggest the overestimation of drag force – the main force responsible for droplet motion and deflecting them from the surface. In a real flow a droplet is likely to distort from the spherical shape and assume a more streamlined shape[8].

In Figure 3 a comparison of the experimental results and the computations for the second test case is presented. In this case the computations were conducted for a single-diameter droplet phase, whereas the experimental results were obtained for a distribution of droplet diameters with median diameter of $236\mu\text{m}$, as the assumed diameter in the computations, but with maximum diameter reaching $1000\mu\text{m}$. In contrast to the previous test case the model of single droplet diameter overpredicts the amount of water captured by the surface. This effect is explained in [4,8] by droplet splashing on the surface in the real flow. The droplets of diameters of more than $50\mu\text{m}$ are termed Supercooled Large Droplets, and are likely to splash when hitting the surface and return a fraction of the water back into the flow. For this reason, a proper splashing model is needed to obtain accurate distribution of the collection efficiency characteristics. However, this result is still valuable from a viewpoint of a design of

anti-icing devices, since the maximum β is predicted correctly. The overprediction of the collection efficiency occurs mainly in the area of low β . From the practical viewpoint of safe design of anti-icing installation the overprediction of the amount of water that reaches the surface is safer than underprediction of it. It is worth noting, that the Supercooled Large Droplet case represents rarely occurring conditions of high water content and droplet diameter in excess of values defined in airworthiness regulations FAR 25 for certification in icing conditions. This type of icing conditions became a field of research in recent years [4,8,9], resulting in propositions of amendments for the airworthiness certification regulations[10].

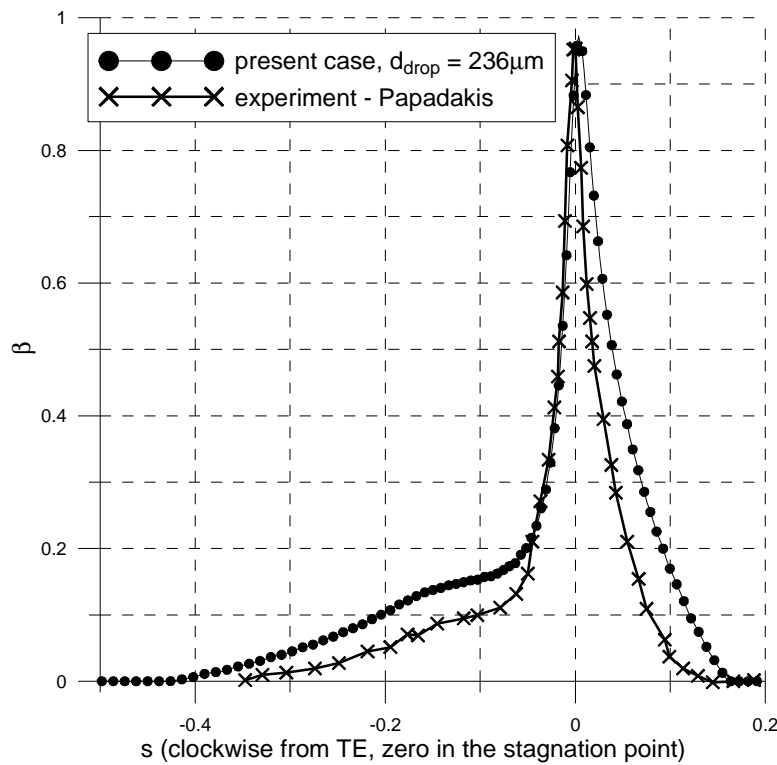


Figure 3. Distribution of the water collection efficiency along the airfoil circumference, second test case.

The airworthiness regulations, FAR25, appendix C [7] define icing conditions in terms of droplet median diameter against liquid water content for different temperature values (Figure 5). It is therefore interesting to compare the results of mass flux of collected water computed for a single-diameter approximation of droplet distribution with results for different distributions of droplet size, since the computations for a single-droplet approximation of the droplet phase flow require much less time and resources than computations for a distribution of droplet size. For this purpose the mass flux of collected water computed for single droplet distributions and conditions defined by $t=-20^{\circ}\text{C}$ and diameter of $20\mu\text{m}$ (Figure 5), was compared with results obtained for three normal distributions of droplet size, each with medium diameter of $20\mu\text{m}$, diameter range of $\langle 0 - 40\mu\text{m} \rangle$ and different values of standard deviation σ (Figure 4).

Mass flux of collected water for a given value of σ was obtained as weighted sum of fluxes computed for each diameter indicated with a dot in graphs of Figure 4, obtained through the integration of the β characteristics over the airfoil surface. The values of the fraction of total LWC corresponding to given β characteristics were used as weighing coefficients. The results of computations are presented in Figure 6. They indicate, that for the determination of mass of water collected by an airfoil, in conditions defined by the FAR 25 regulations (Figure 5) a single-diameter droplet distribution model is justified.

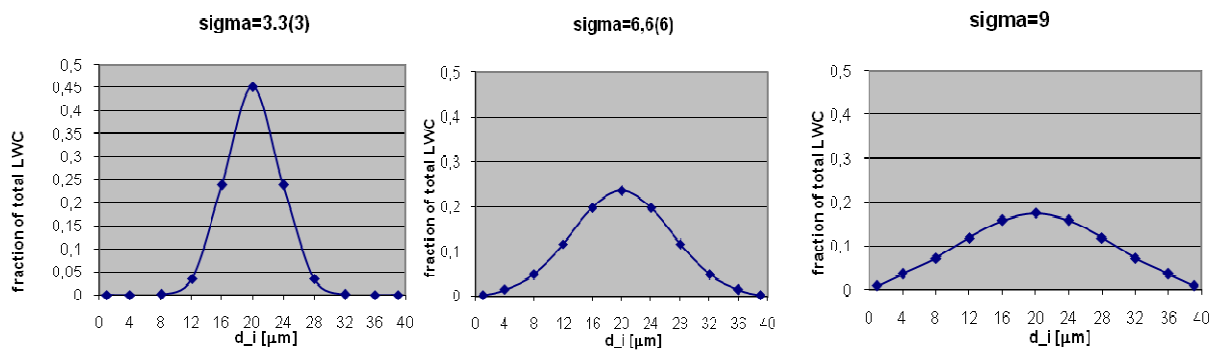


Figure 4 Distributions of droplet diameter.

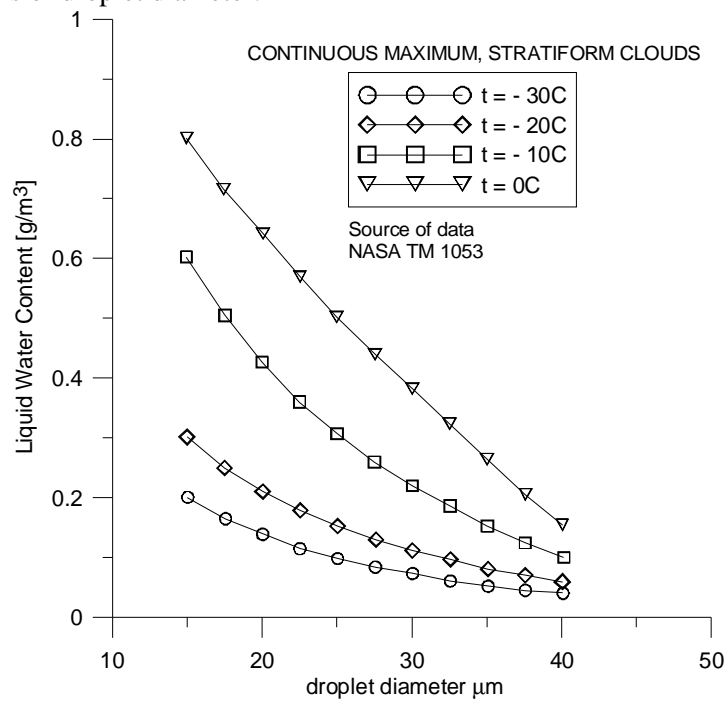


Figure 5. Definition of continuous icing conditions, FAR25 regulations, appendix C.

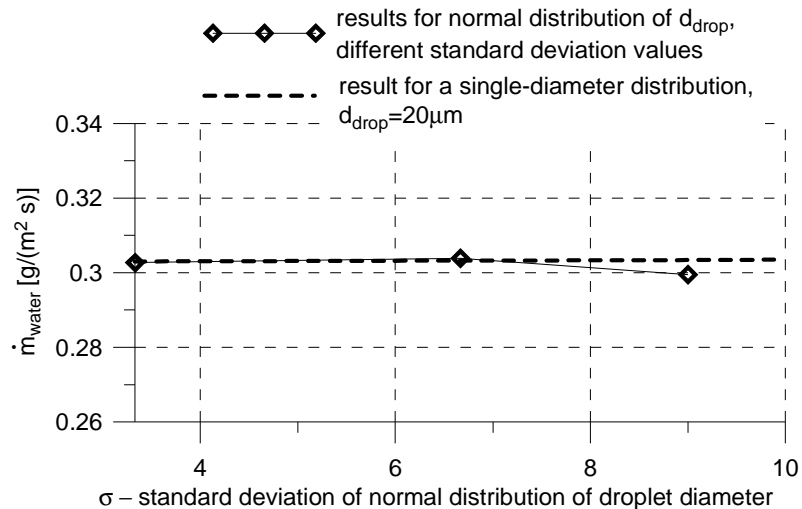


Figure 6. Mass flux of water collected by airfoil at different values of σ . NACA 23012 airfoil at $\alpha=2.5^\circ$, $M=0.22$, $Re=4.5\text{mln}$, $LWC=0.2\text{g/m}^3$.

For the icing conditions defined in Figure 5 computations were performed to determine the values of diameters of droplet captured most likely by an airfoil. The results, presented in Figure 7 show, that at temperatures between 0°C and -10°C the most likely to hit an airfoil are droplets of diameters between 20 and 30µm. At low temperatures, close to -20°C the mass of collected water is more independent of droplet diameter.

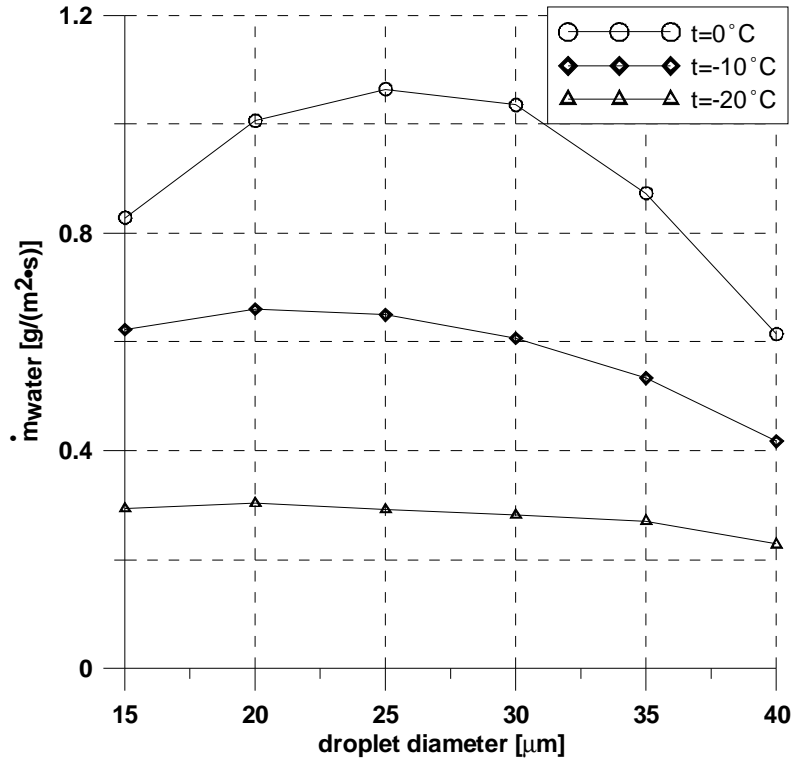


Figure 7. Dependence of mass of collected water on droplet diameter for icing conditions defined by FAR 25 regulations, Appendix C. NACA 23012 airfoil at $\alpha=2.5^\circ$, $M=0.22$, $Re=4.5$ mln.

Investigations of the effect of flight parameters: angle of attack and Mach number on the mass of collected water were also conducted. Computations for different values of angle of attack were done for NACA 23012 airfoil at Mach number of 0.22 and Reynolds number of 4.5 mln using single-diameter approximation for the droplet phase. Figure 8 shows distributions of the collection efficiency β computed for the range of angle of attack values from 2.5° to 11° . A tendency of decreasing the peak value and increasing the area hit by the droplets as the angle of attack is increased is visible. Also the point of peak value of β moves slightly towards the bottom side of the airfoil, following the stagnation point. In Figure 9 dependence of the mass flux of collected water on the angle of attack is shown. The results were obtained for two conditions of temperature and Liquid Water Content, according to FAR 25, app C: 0°C , 0.19g/m^3 and -20°C , 0.635g/m^3 . In both cases the angle of attack of minimum collected water coincides approximately with minimum of profile drag. There is no rapid growth of the mass of the collected water when angle of attack is increased within the investigated α -range. Mass flux of collected water at $\alpha=11^\circ$ is approximately 30% higher than its minimum at $\alpha=1\sim 2^\circ$. Figure 10 shows the effect of Mach number change on the mass of collected water and maximum value of β . The computations for Mach number range of 0.2 to 0.5 reveal, that collection efficiency increases with growing Mach number, which is the reason for faster than linear growth of the mass flux of collected water. This effect should be taken into account in the design of anti-icing installations.

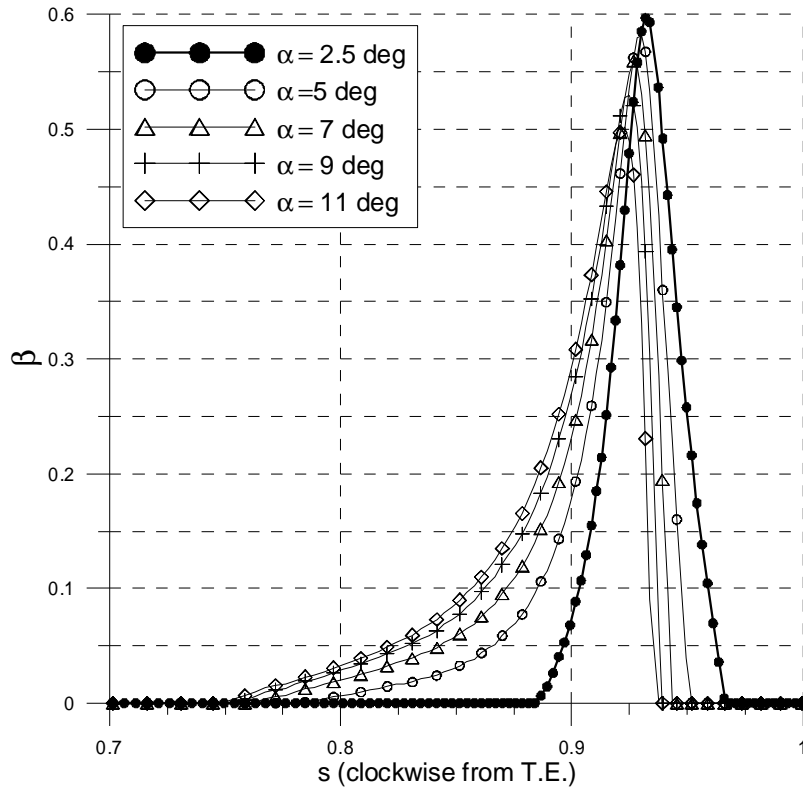


Figure 8. Water collection efficiency characteristics obtained for different angles of attack for NACA 23012 airfoil at $\alpha=2.5^\circ$, $M=0.22$, $Re=4.5\text{mln}$. $LWC=0.2\text{ g/m}^3$, $t=-20^\circ\text{C}$, $d_{\text{drop}}=20\mu\text{m}$.

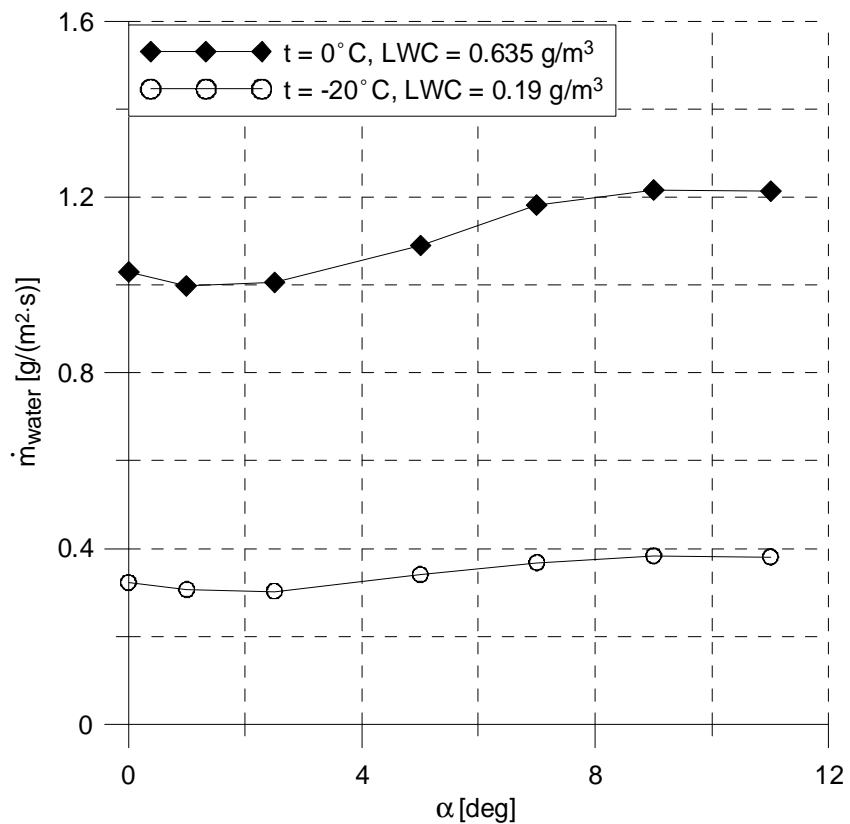


Figure 9. Dependence of mass flux of collected water on the angle of attack for two sets of icing conditions. Results obtained for NACA 23012 airfoil at $\alpha=2.5^\circ$, $M=0.22$, $Re=4.5\text{mln}$. $LWC=0.2\text{ g/m}^3$, $t=-20^\circ\text{C}$ and $t = 0^\circ\text{C}$.

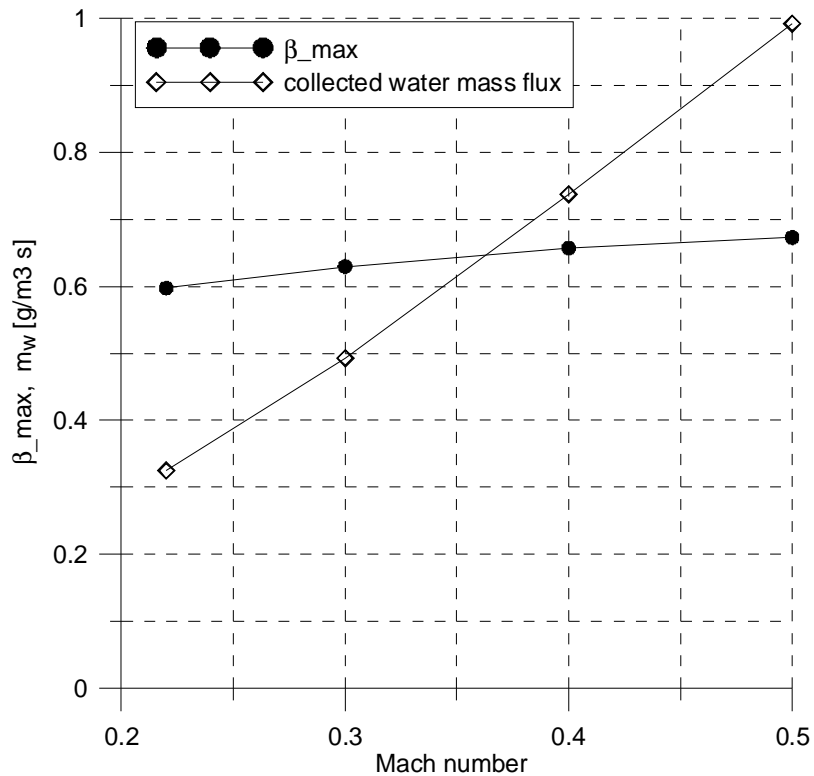


Figure 10. Dependence of the maximum value of collection efficiency β and mass flux of collected water on Mach number. Results obtained for NACA 23012 airfoil at $\alpha=2.5^\circ$, LWC=0.2 g/m³, $t=0^\circ\text{C}$.

CONCLUSIONS AND FUTURE WORK

A model of low-density droplet phase flow was developed and implemented in the FLUENT solver. Two experimental test cases were used to validate the model. The first test case represented flow conditions typical for small droplet, low Liquid Water Content, described by the FAR 25, Appendix C regulations – conditions of continuous icing in stratiform clouds, the second test case was representative of Supercooled Large Droplets. The water collection efficiency β characteristics computed with the present method are close to the characteristics obtained in experiment, with differences mainly in areas of low values of the β parameter. In the first case of small droplets the present method slightly underestimates the collection efficiency, and in the second case the method overestimates it. The most likely reasons are the neglected effects of droplet deformation and splashing, which, particularly for large droplets leads to reintroduction of a fraction of water into the flow. The computations for different shapes of normal distribution of droplet diameter distribution were aimed at exploring the possibility of using single droplet diameter for the determination of mass flux of collected water. Results of Mass flux of collected water obtained for single diameter distribution and for normal distribution of droplet diameters with standard deviation of 1/6 of the assumed diameter range (a frequently applied model of normal distribution for random variations in technology) were practically identical. Comparison of mass flux of collected water obtained for different droplet diameters revealed, that for high water concentration in the cloud the most likely to collide with airfoil are droplets of diameter approximately in the middle of the range defined by FAR 25 regulations for aircraft certification in icing conditions. For low values of water concentration the mass flux of collected water is more independent of droplet diameter. Computations for different values of angle of attack, within the range of its normal takeoff/landing, cruise values revealed that the lowest rate of

water collection occurs at low profile drag values of angle of attack, without rapid growth at higher alphas. Increasing Mach number leads to mild increase of the collection efficiency which is responsible for faster than linear growth of the mass flux of collected water with increasing Mach number.

Future work in this field will be directed towards the development of models for water film transport on the surface which will enable the solution of energy balance equations on the surface in icing conditions, and in consequence, determination of ice accretion rate.

REFERENCES

- [1] Potapczuk M.G., Al-Khalil K.M., Velazquez M.T., *Ice Accretion and Performance Degradation Calculations with LEWICE/NS*, NASA Technical Memorandum 105972, AIAA-93-0173, Prepared for the 31st Aerospace Sciences Meeting and Exhibit, Reno, Nevada, January 11-14, 1993.
- [2] Beaugendre H., Morency F., Habashi W.G. *FESNSAP-ICE's Three-Dimensional In-Flight Ice Accretion Module: ICE3D*, Journal of Aircraft, Vol 40, No.2, March-April 2003.
- [3] FLUENT 6.3 User's Guide, Fluent Inc.2006.
- [4] Hospers J.M., Hoeijmakers H.W.M., *Numerical Simulation of SLD Ice Accretions*, 27th International Congress of the Aeronautical Sciences, 2010.
- [5] Morrison F.A., *Data Correlation for Drag Coefficient for Sphere*, Department of Chemical Engineering, Michigan Technological University, Houghton, MI, www.chem.mtu.edu/~fmorriso/DataCorrelationForSphereDrag2010.pdf, accessed October 2011.
- [6] Papadakis M, Rachman A, Wong S.-C, Yeong H.-W, Hung K. E, Vu G. T, and Bidwell C. S. *Water droplet impingement on simulated glaze, mixed and rime ice accretions*. Technical Report NASA/TM-2007-213961, NASA, October 2007.
- [7] Federal Aviation Regulations FAR 25 Appendix C, http://www.flightsimaviation.com/data/FARS/part_25-appC.html
- [8] Hospers J.M., Hoeijmakers H.W.M., *Eulerian Method for Ice Accretion on Multiple-Element Airfoil Sections*. In: 2ND FERMaT-IMPACT Meeting, 13-16 October 2009, Enschede, the Netherlands
- [9] Jentink H.W. *Supercooled large droplets in icing conditions*, NLR-TP-98216
- [10] Newton D. *What's Ahead in Icing Certification*, Aviation Week, Oct 1, 2010, http://www.aviationweek.com/aw/generic/story_channel.jsp?channel=bca&eventName=coldops2010&id=news/coldops1010p17.xml